ISSN 0717-652X

MODES OF INTERANNUAL VARIABILITY OF OCEANIC EVAPORATION OBSERVED FROM GSSTF2

Long S. Chiu[1] & Yukun Xing

SCS/CEOSR, George Mason University, Fairfax VA 22030 U.S.A.
lchiu@gmu.edu, yxing@gmu.edu and Alfred T-C. Chang
1. NASA/GSFC, Code 974, Greenbelt Maryland 20771, U.S.A.

ABSTRACT

Variations of the oceanic evaporation are examined using Goddard Satellite Surface Turbulence Flux version 2 (GSSTF2) data. An Empirical Orthogonal Function (EOF) analysis shows that the first non-seasonal EOF, which explains 9.2% of the variance, is characterized by large changes in the subtropical oceanic dry regions, accompanied by small negative changes in the equatorial warm pool and the eastern equatorial Pacific. The time series shows an increasing trend with decadal time scale that started around 1990. This pattern is interpreted as an enhancement of the Hadley and Walker circulation. The second EOF, explaining 5.7% of the variance, is characterized by an equatorial east-west and a mid ocean north-south dipole in the Pacific. The second pattern is similar to the First EOF pattern of non-seasonal oceanic precipitation found in earlier studies, and is related to the El Nino Southern Oscillation phenomena. It is correlated with a Southern Oscillation Index at 0.74, which is significant at the 95% level. Over the region 65^0S – 65^0N, oceanic evaporation, surface wind speed and air-sea humidity difference from GSSTF2 shows increases of 17%, 6% and 11% over the period July 1988-December 2000. Most of this linear trend is associated with a decadal variation of the atmospheric circulation and points to the need for quantifying interannual variations in long-term climate changes studies in the global hydrologic cycle.

INTRODUCTION

Oceanic evaporation is a key component of the global hydrologic and energy cycles. Over the global oceans, excess evaporation over precipitation (E-P) is balanced by increase continental runoff. If the terrestrial, atmosphere and oceanic reservoirs remain unchanged, continental runoff must be balanced by atmospheric moisture transport from over the oceans to over land. Hence the spin up of the hydrologic cycle will be manifested in variations of oceanic evaporation over precipitation, increase river runoff and moisture convergence over the continents.

Oceanic evaporation is a key component of the ocean surface heat balance. Because of the saturated underlying surface, evaporation is radiation limited: the maximum being determined by the net radiation. In a bulk aerodynamic formulation, it is determined by factors such as the moisture gradient at the air-sea interface, surface wind, sea state, and atmospheric stability. Hence, evaporation responds to atmospheric circulation changes, such as that due to cloudiness changes affecting the net radiation balance, variations of the zonal or meridional circulation that affects the surface stresses, and dehydration of the lower atmosphere due to large scale atmospheric sinking motions. Increased evaporation provides the energy source that can trigger or intensify cyclone and hurricane formation. It is therefore both a diagnostic and prognostic tool for the atmospheric and oceanic circulation.

There is an on-going debate about the coupled modes of ocean-atmosphere interaction from satellite records. Chen et al. (2002) and Wielicki et al. (2002a) examined the TOA radiative budget between 30^0S and 30^0N and suggest that there are increases in longwave cooling and short wave absorption during the recent period. Cess and Udelhofen (2003) extended the analysis to the region 40^0S to 40^0N and found similar conclusions. They suggest that these changes are part of the decadal variation of the Hadley circulation that started in around 1990. They concluded that changes in longwave and shortwave fluxes are consistent with a decadal intensification of the tropical Hadley and Walker circulation that recently started around 1990. Concerns about the inter-satellite calibration and

satellite sampling have been raised (Trenberth, 2002) in interpreting these results. Wielicki et al. (2002b) analyzed errors in the satellite estimates and concluded that the interdecadal mode is not pure noise.

While cloud and radiation records are determined from visible and IR observations, satellite microwave remote sensing has been used to derive various oceanic parameters, such as sea surface temperature, surface wind, and moisture. These parameters have been used to compute ocean surface flux estimates. Does the microwave record also show the decadal mode found in the visible/IR observations?

In order to examine long-term climate trends in the global hydrologic cycle, an understanding of the sub-annual and interannual variations are necessary. In this study, we report on an EOF analysis of the interannual variability of global evaporation from satellite microwave observations. The factors that control the temporal and spatial variations are examined to interpret the interannual modes.

DATA

We can broadly classify two approaches to global evaporation estimation, remote sensing and model re-analyses. The SEAFLUX project has put together surface flux data sets for comparison (Curry et al., 2003). Remote sensing from space-borne platforms provides the means to monitor evaporation over the vast oceans. The Goddard Satellite-based Surface Turbulent Flux Version 2 (GSSFT2) data set (Chou et al. 1995, 1997) is used in this study as it has the longest temporal coverage among the satellite data sets. Chou et al. (2003) validated the GSSTF2 against hourly observations from nine field experiments and found a bias of 0.8 Wm^{-2} (standard error of 35.8 Wm^{-2}) and for all nine experiments and -2.6 Wm^{-2} (SD = 29.7 Wm^{-2}) for the five experiments in the tropics. Chou et al. (2004) compared the GSSTF2 fluxes with the Hamburg Ocean Atmosphere Parameters and Fluxes from Satellite Data (HOAPS), NCEP reanalysis and the De Silva et al. (1994) surface marine analysis for 1992-1993 and concluded that "the GSSTF2 latent heat flux, .." are likely to be more realistic than the other data sets, "although it is subjected to regional biases."

The Version 2 of the Goddard Satellite based Surface Turbulent Fluxes (GSSTF-2) Data Set contains 1^0 by 1^0 daily, monthly and monthly climatology of latent heat flux, sensible heat flux, surface (10-m) air specific humidity (Q), lowest 500-m precipitable water (WB), 10-m wind speed (U), sea-air humidity difference, zonal and meridional wind stresses from 90^0N to 90^0S. The parameters are derived from Special Sensor Microwave Imager (SSM/I) measurements. Our analysis focuses on the areas between 65^0N and 65^0S. The latent heat flux is based on bulk aerodynamic formulation (Chou et al. 1995, 1997) using the 10-m wind speed and sea-air humidity difference. The surface air humidity is derived from the vertical humidity profile fitted using the columnar and boundary layer water vapor. A monthly value is produced only when more than 10 days of daily data are available for a particular month. The evaporation data can be computed from latent heat, i.e., $LH = \tilde{n}_w \cdot \ddot{e}_v \cdot E$, where LH is the latent heat flux (W/m^2), $\tilde{n}_w$ is the mass density of water (g/m^3), E is the evaporation rate (m/s), and $\ddot{e}_v$ is the latent heat of vaporization (J/kg^1).

Figure 1 shows the number of months available for our analysis. Missing data can be either due to instrument error, or due to the non- retrieval of parameters (e.g. surface air specific humidity) in the presence of heavy rain. In most part of the ocean, the number of missing months is less than 2 (out of 161, or around 1%). The regions with the largest number of missing data (>5%) are located in the Bay of Bengal and part of the Arabian Sea. The heavy rain regions, such as the Inter-Tropical Convergence Zone (ITCZ), the maritime continent, South-China Sea and part of the western tropical Pacific show typically less than 5% missing months. The temporal distribution of missing data at 20-degree latitude belts were examined and no apparent trends in the number of missing data is found.

ANALYSIS AND RESULTS

An EOF analysis is performed on the anomalies (with monthly climatology removed) of the latent heat flux data from January 1988 to December 2000 (Essenwagner, 1976). The first two EOFs are significant and distinct according to the tests proposed by North et al. (1982). Figure 2 shows the EOF patterns. Their associated time series are shown in Figure 3. The time series of the first EOF in the figures have been re-scaled for better visualization effects.

The first EOF, which contributes 9.2% to the total variances, has a spatial pattern that is characterized by large areas of positive changes in the subtropical Pacific and Indian oceans, accompanied by negative

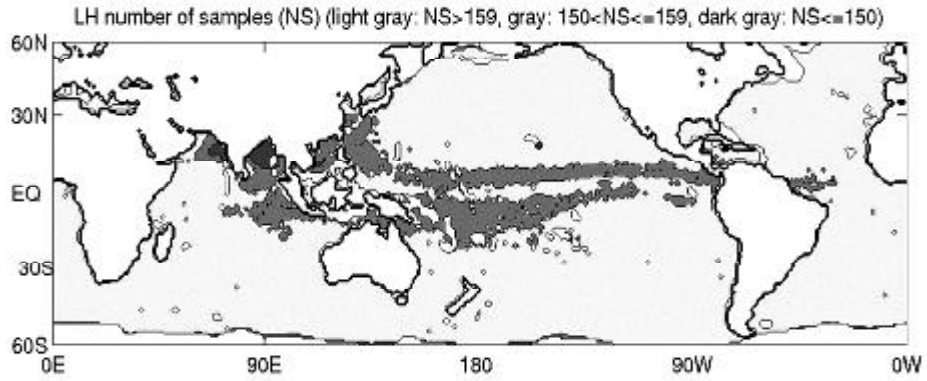

FIGURE 1: Available monthly latent heat flux data July 1987- December 2000

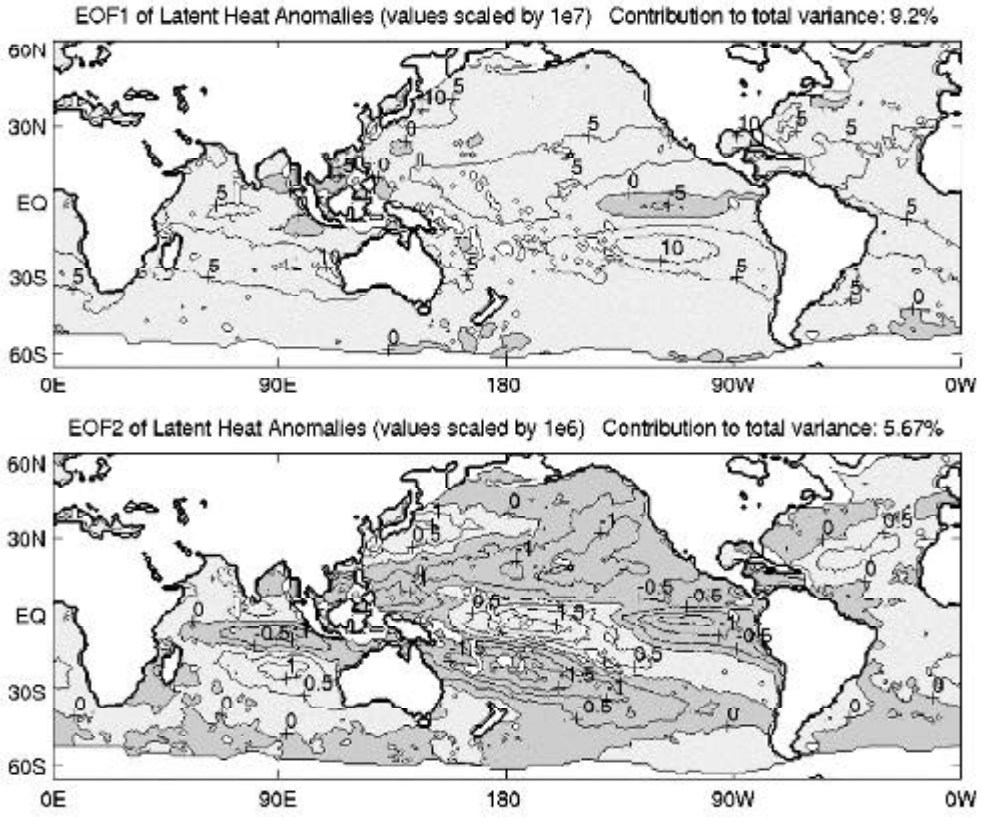

FIGURE 2: The first EOF (upper panel) and second EOF (lower panel) patterns of latent heat flux anomalies. Areas with positive values are shaded in light gray, areas with negative values are shaded with dark gray, and areas with no available data are in white. "+" sign in the plot indicates the labeling of the contour line.

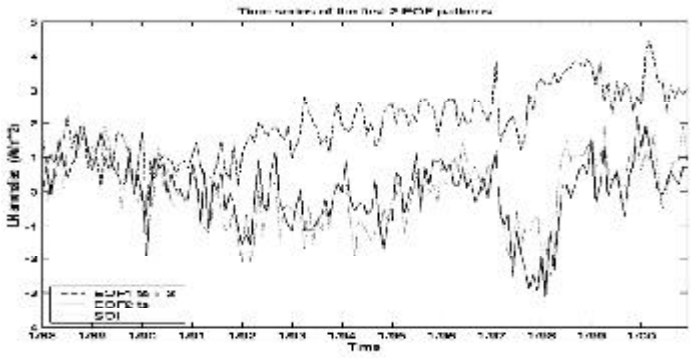

FIGURE 3: Time series of the first two EOF and SOI. The time series of EOF1 is shifted up by 2 units for clarity. Correlation between SOI and EOF2 time series is 0.74, significant at the 95% level.

changes over eastern equatorial Pacific and the maritime continent. The time series of EOF1 shows an increase that starts around 1990. We performed an Empirical Mode Decomposition (EMD) of the first time series (Huang et al., 1998) (results not shown). The longest time scale Intrinsic Mode Function (IMF) shows an increasing function that starts increasing around 1990.

Evaporation is mostly determined by surface wind (U) and air-sea humidity difference (DQ). To help interpret the results, we computed the weighed sum of the monthly fields of U and DQ from GSSTF2 by the time series of the EOF1. The results of the EOF1-U mode show striking similarity to the EOF1 of evaporation, with large positive areas in the tropical central Pacific, the subtropics in both the Pacific and Indian Ocean, accompanied by negative values in the eastern equatorial Pacific and the maritime continent. The EOF1-DQ modes shows large zonal negative changes in the tropical Pacific accompanied by large positive changes in the subtropics in both Pacific and the Indian Ocean. The EOF1-DQ pattern can be interpreted as an enhanced Hadley and Walker circulation. At the rising branch of the Hadley circulation near the equator, the convergence of moisture increase surface air humidity (Q_a) and hence decreases the air-sea humidity difference (DQ= Qs-Qa). In the sinking branch of the Hadley circulation, sinking air brings dry air from aloft and decreases Qa and hence increases DQ.

The second EOF pattern contributes 5.7% to the total variances. It is characterized by strong dipole structures. Large positive anomalies in the central equatorial Pacific, from about 160^0E to 135^0W and extends southeastward to the coast of South America, are associated with large negative anomalies over the South Pacific Convergence Zone that centers at 20^0S, 175^0W. Other negative centers are in the maritime continents and the eastern equatorial Pacific. There is a northwest/southeast dipole in the north Pacific. Over the Indian Ocean, there is meridional positive-negative-positive pattern, corresponding to the north, equatorial and subtropical south Indian Ocean. This global pattern is very similar to the ENSO patterns of non-seasonal precipitation from SSM/I found in earlier studies (Chang et al. 1993; Kafatos et al. 2001). The time series of the second EOF shows a correlation of 0.74 with SOI. The SOI used here is that provided by the Climatic Research Unit of University of East Anglia, UK. The correlation is significant at 95% confidence level. The effective number of samples is estimated from the autocorrelation of the two time series (Angell, 1981). Based on the spatial pattern and temporal characteristics, it is concluded that the second EOF is indicative of ENSO events. The correlation between SOI and the first EOF time series is 0.26, which is insignificant by the same test.

We examine linear trends in the global average (65^0S and 65^0N) of the GSSTF2 oceanic evaporation. There is an increasing trend in the global averages of oceanic evaporation of 0.66 mm/day vs. the 1987-2000 mean of 3.87 mm/day or 17% (1.2%/year) increase. The increases in global average U is 0.43 m/s vs. a mean of 7.40 m/s (about 6% increase) and DQ increase of 0.45 g/kg vs. a mean of 4.16 g/kg (11% increase).

SUMMARY AND DISCUSSION

An EOF analysis of the GSSTF2 latent heat flux shows two significant and distinct modes of non-seasonal variability. The first EOF contributes 9.2% to the total variances. This pattern is consistent with an enhanced Hadley and Walker Circulation as suggested by Chen et al. (2002), Wielicki et al. (2002a), and Cess and Udelhofen (2003). The strengthening of the Hadley and Walker circulation moistens the convective regions and dries the subsidence regions hence they imply increases in cloudiness in the regions of rising motion and decreases in the subsidence regions. We have examined trends in the sensible heat flux in the same data set and found similar trends. While short wave absorption associated with increased cloudiness decreases the surface radiative budget, the effect on the upward longwave flux is of opposite sign. A full assessment of the influence of the tropical circulation on surface heat fluxes must await further analysis of the surface radiative, dynamical and turbulent energy fluxes.

The second EOF, which explains 5.7% of the variance, has a very clear dipole structure, where the positive center is located over the western and central Pacific and the negative center is located over the southwest Pacific. The time series of the second EOF has a very high correlation with an SOI index. Both the spatial and temporal variations suggest clearly that this is an ENSO mode. It is thus concluded that the GSSTF product is capable of deciphering one of the most significant inter-annual variation mode.

Linear trend analysis of global oceanic evaporation of the GSSTF2 data set shows an increase of 17% over the period July 1987 to December 2000. This increase is accompanied by a 6% increase in global wind speed and 11% in air-sea humidity difference. The significance of these "trends" must be examined in light of the uncertainty of the components. From our analysis, it is shown that most of the linear trends are associated with an enhanced Hadley circulation. Our results, therefore, point to the need to examine interannual variations, such as ENSO and decadal Hadley circulation variations, in addition to error estimates of these parameters, to quantify long-terms variations of the global hydrologic cycle.

ACKNOWLEDGMENTS

Dr. Alfred Chang passed away during the course of this work. His leadership, encouragement and friendship will be sorely missed. This work is partially supported by NASA Office of Earth Sciences, Tropical Rainfall Measuring Mission.

REFERENCES

ANGELL, J. K., 1981: Comparison of variations in atmospheric quantities with sea surface temperature variations in the equatorial eastern Pacific, *Monthly Weather Review, 109*, 230-243. [1]

CESS, ROBERT D., UDELHOFEN, P. M., Climate change during 1985-1999: Cloud interactions determined from satellite measurements, *Geophysical Research Letter*, 30, 1019-1022, 2003. [2]

CHANG, A. T-C., L. CHIU, & T. T. WILHEIT, 1993: Oceanic Monthly Rainfall Derived from SSM/I, *Eos Transaction AGU, 74*, 505–513. [3]

CHEN, J., B. E. CARLSON, & A. D. DEL GENIO, 2002: Evidence for strengthening of the tropical general circulation in the 1990s, *Science*, 295 (5556), 838-841. [4]

CHOU, S-H,, R. M. ATLAS, C-L. SHIE & J. ARDIZZONE, 1995: Estimates of Surface Humidity and Latent Heat Fluxes over Oceans from SSM/I Data, *Monthly Weather Review, 123*, 2405-2425. [5]

CHOU, S-H,, C-L. SHIE, R. M. ATLAS, J. ARDIZZONE, 1997: Air-sea Fluxes Retrieved from Special Sensor Microwave Imager Data, *Journal of Geophysical Research, 102*, 12705-12726. [6]

CHOU, S-H., E. NELKIN, J. ARDIZZONE, R. M. ATLAS, & C-L. SHIE, 2003: Surface turbulent heat and momentum fluxes over global oceans based on the Goddard satellite retrieval, version 2 (GSSTF2). *Journal of Climate*, 16, 3256-3273. [7]

CHOU, S-H., E. NELKIN, J. ARDIZZONE, & R. ATLAS, 2004:A comparison of latent heat fluxes over global oceans for four flux products, *Journal of Climate* (to appear). [8]

CURRY, J. & COAUTHORS, 2004: SEAFLUX, *Bulletin of the American Meteorological Society*, 85 (3), 424. [9]

ESSENWAGNER, O., 1976: Applied statistics in atmospheric sciences, Part A: Frequencies and curve fitting. In Development in atmospheric sciences, 4A, Elsevier, 252-275. [10]

HUANG, N. E., Z. SHEN, S. R. LONG, M. C. WU, H. H. SHIH, Q. ZHENG, N-C. YEN, C. C. TUNG, H. H. LIU, 1998: The empirical mode decomposition and the Hilbert spectrum for nonlinear and non-stationary time series analysis, *Proceedings of the Royal Society*, Lond., 454A, 903-995. [11]

NORTH, G. R., BELL, T. L., CAHALAN, R. R., 1982: Sampling errors in the estimation of empirical orthogonal functions, *Monthly Weather Review, 110*, 699-706. [12]

TRENBERTH, K., 2002: Changes in tropical cloud and radiation, *Science*, 296 (5576), 2095. [13]

WIELICKI, B., T. WONG, R. P. ALLEN, A. SLINGO, J. T. KIEHL, R. J. SODEN, C. T. GORDON, A. J. MILLER, S-K YANG, D. A. RANDALL, F. ROBSERTSON, J.

SUSSKIND, AND H. JACOBOWITZ, 2002(a): Evidence for large decadal variability in the tropical mean radiative energy budget, *Science*, 295 (5556), 841- 844. [14]

WIELICKI, *et al*., 2002(b): Response, *Science*, 295, 841. [15]